

Magnetoresistance when Spin Effects on Conduction are Weak

Vincent Sacksteder IV*

Department of Physics and Astronomy, Rutgers University, NJ, USA

This paper considers certain materials, including topological insulators, where spin rotation symmetry is broken much more strongly than time reversal symmetry. When these materials are in the diffusive regime, i.e. when they have disorder that is strong enough to cause an electron to scatter many times while crossing a sample, electrons and holes move in pairs that have zero spin and are insensitive to spin physics. Working within this spinless scenario, we show that Fourier transforming the magnetoconductance with respect to external magnetic field obtains a curve describing the area distribution of loops traced by electrons and holes within the sample. We present loop area distributions of Landau levels, weak (anti)localization, conduction governed by Levy flights, and linear-in-field resistance. Of these four the last two are new results. Comparing these distributions, we argue that the linear-in-field resistance seen in some topological insulators is caused by the same diffusive scattering that causes weak antilocalization. The difference is that linear-in-field resistance materials retain a level of quantum coherence that is usually seen only on the surface of 2-D wires or in ring geometries. In an appendix we include some speculative material about linear-in-temperature resistance.

PACS numbers: 72.15.Rn, 73.23.-b, 71.27.+a, 74.72.Kf

In atomic units $m_e = e = \hbar = k_B = 1$ the magnetic field B has dimensions of inverse area, which is key to understanding the electrical conductance's dependence on B . Large fields probe areas at the scale of the unit cell, and small changes in field probe much larger areas. At large fields one finds Landau levels and Schubnikov-de Haas (SdH) oscillations, which are visible in the longitudinal conductance $G_{xx}(B)$ as peaks at characteristic field strengths determined by the Fermi energy E_F . The Fermi surface's cross section, an inverse area, can be read off from the peak positions. Landau levels and SdH oscillations are signals of ballistic physics, i.e. weak scattering, and are extinguished once scattering becomes too frequent.

At small fields one finds weak (anti) localization (WL/WAL), where scattering and quantum interference cooperate to cause G_{xx} to decrease or increase with field depending on whether spin rotation symmetry is broken faster or slower than time reversal symmetry. WL/WAL contrasts strongly against Landau levels and SdH oscillations. It is much more sensitive to magnetic field, is visible at much smaller field strengths, and varies smoothly with field rather than exhibiting oscillations. Moreover WL/WAL is caused by physics at length scales much longer than the scattering length. It is only weakly sensitive to the atomic unit cell and the Fermi wavelength.

Recent years have exposed mysteries which lie well beyond traditional SdH and WL/WAL physics. Many experiments report systems where the longitudinal resistance R_{xx} increases linearly with B and does not saturate.^{1–11} This contrasts both with SdH oscillations which oscillate periodically in $1/B$ and with WL/WAL which is logarithmic. Explanations have been given for the cases of ballistic conduction when the Fermi surface has a cusp, of a 3-D Dirac cone in the presence of a strong magnetic field, of a density gradient across the sample, and of classical transport with strong sample

inhomogeneities.^{12–16} However this kind of case by case treatment is not entirely satisfactory given the wide range of experimental realizations.

The electrical conductance is determined by electrons and holes. Magnetic field affects electrons and holes in two ways. The first is the minimal coupling $\vec{p} - e\vec{R}$, where \vec{R} is the gauge field determining the magnetic field by $\vec{B} = \vec{\nabla} \times \vec{R}$. This coupling is sensitive only to a fermion's kinetics, not its spin. In contrast, the $e\vec{\sigma} \cdot \vec{B}$ Zeeman term provides a very direct coupling between field and spin. The Zeeman term is accompanied by similar terms which are of higher order in momentum \vec{p} , electric field \vec{E} , and magnetic field.¹⁷

In this paper we concern ourselves with materials where the Zeeman term's effect on conduction can be neglected, leaving in play only the minimal coupling. In other words, we confine ourselves to systems where electronic conduction is mediated by spin singlets; we explore where this simplification can lead us. Always working under the assumption that the Zeeman term can be neglected, we show that external magnetic field is conjugate to the area of the electron-hole loops inside a material. In non-interacting systems the conjugate area is that of a single loop, and in interacting systems it is the sum of the areas of all loops contributing to the conductance. Therefore if one analyzes the magnetoconductance by taking the Fourier transform with respect to external magnetic field, one can extract detailed information about the length and area scales in play in electronic conduction within the material. We apply this methodology to Landau levels, SdH oscillations, and weak antilocalization. We go on to see what this methodology says about materials with linear-in-field magnetoresistance, if their linear resistance is caused by the minimal coupling not the Zeeman term. Lastly we include some more speculative material concerning materials displaying linear-in-temperature resistance.

There exist many materials where electronic conduction is determined by spin singlets only; in these materials the spin triplet and the Zeeman effect have no influence. There are two ingredients for obtaining this scenario. First, the material should be in the diffusive regime, where the scattering length is much shorter than the sample size. Second, spin rotation symmetry must be broken more strongly than time reversal symmetry, as is the case with strong spin-orbit coupling.

The first ingredient for spin-singlet conduction is diffusive conduction, with many scatterings as electrons and holes traverse a sample. At lengths exceeding the scattering length l the electronic wave-function $|\psi\rangle$'s phase is randomized, rendering single wave-functions unable to mediate conduction. Therefore conduction over distances longer than l is mediated only by pairing between $|\psi\rangle$ and its complex conjugate $\langle\psi|$, whose random phases cancel. This pairing produces the single-particle density matrix $\rho(x)$, which is the key mediator of conduction at distances longer than the scattering length. This result is well known from the extensive work on sigma models and bosonization techniques in disordered systems.^{18,19}

ρ 's evolution is sensitive only to processes where $|\psi\rangle$ and $\langle\psi|$ undergo the same scattering events and follow the same path between scatterings, because only these processes satisfy the requirement that the disorder-induced random phases of $|\psi\rangle$ and $\langle\psi|$ must cancel. There are two such processes, the diffuson and the Cooperon. In the diffuson $|\psi\rangle$ and $\langle\psi|$ follow the same sequence in the same order, producing purely classical electronic motion. In contrast the Cooperon is a quantum interference process, distinct from classical motion. In the Cooperon $|\psi\rangle$ and $\langle\psi|$ follow the same sequence but in reversed order, and their phases seem to be randomized with respect to each other. It is not until their trajectories close a loop and come back to their origin that $|\psi\rangle$ and $\langle\psi|$'s phases suddenly cancel and $\rho(x)$ undergoes a revival. Comparing the diffuson and the Cooperon, the diffuson is purely classical and depends weakly on magnetic field, while the Cooperon is purely quantum mechanical and is strongly dependent on even very weak magnetic fields.

The main effect of spin on disordered transport is that $\rho(x)$ contains both a spin singlet (charge) and a spin triplet (spin polarization). Both the spin singlet and the spin triplet have characteristic relaxation times τ_s and τ_t that are determined by the material and by embedded impurities. When the spin singlet relaxes more slowly than the spin triplet, i.e. when $\tau_s \gg \tau_t$, then the spin singlet contribution dominates and the spin triplet's contribution to conduction is negligible. This combination of lifetimes $\tau_s \gg \tau_t$ is found when spin rotation symmetry is broken more strongly than time reversal symmetry. This is the case in materials with strong spin-orbit coupling, including topological insulators. In particular, when topological insulators are in the diffusive regime and their charge carriers are from the Dirac cone not from other bands, then conduction is mediated only by spin singlets, not spin triplets.

If the Cooperon increases the conductance when the magnetic field is zero, then its effect is called weak antilocalization (WAL). If on the other hand the Cooperon decreases the conductance at zero field, then this is called weak localization (WL). WAL results in the resistance increasing with field, while WL results in the resistance decreasing with field. Whether weak localization is seen in a material, or instead weak antilocalization, is determined by whether the Cooperon triplet is present.

Magnetic field is a perfect diagnostic tool for distinguishing between systems where the Cooperon spin triplet is absent and ones where it is present. When the Cooperon spin singlet relaxes more slowly than the spin triplet (as in topological insulators), i.e. when $\tau_s \gg \tau_t$, the singlet produces weak antilocalization (WAL), which means that the resistance increases with field. On the other hand, when time reversal symmetry is not more favored than spin rotation, and the spin singlet and spin triplet relaxation time scales $\tau_s \sim \tau_t$ are similar, then the spin triplet dominates and the resistance decreases with field, which is called weak localization (WL).^{20,21} In summary, WAL occurs when the spin triplet relaxes quickly so that conduction is mediated by charges which effectively have zero spin²², while WL occurs when both the spin singlet and spin triplet contribute to conduction.

Experimentally, if the resistance increases with small fields in a diffusive material then only the Cooperon spin singlet is active in conduction, and not the Cooperon spin triplet. If, on the other hand, the resistance decreases with small fields then both the spin singlet and the spin triplet are in play.

Many materials displaying linear magnetoresistance do conduct only via the Cooperon spin singlet, not the spin triplet. Certainly topological insulators lie in this regime, as do Dirac semimetals with strong spin-orbit coupling.¹⁻⁴ Possibly other linear resistance materials, besides TIs and Dirac Weyl materials, may also have negligible spin triplet conduction. Experimental observations of linear magnetoresistance universally find that resistance increases rather than decreases with field, as seen in WAL. Observations of resistance increasing with field are consistent with a short spin triplet relaxation time τ_t and a significantly longer spin singlet lifetime τ_s , and with dominance of spin singlet conduction.

A. Loops and Magnetic Field

This paper develops a geometrical analysis of magnetotransport in terms of the loops traced by electrons and holes as they move through real space. In spin singlet materials where only the minimal coupling and not the Zeeman term couples magnetic field to electrons, electron-hole loops are controlled via the magnetic flux through them and by the Aharonov-Bohm effect. Because magnetic flux is equal to the product of field with loop area, field is conjugate to area. We will develop this fact into a methodology for analyzing experimental measurements

of the conductance.

The starting point of our analysis is Feynman's formulation of quantum mechanics as a sum over paths.²³ In this formulation an electron follows not just one path, but instead many paths which fully explore the sample in which the electron is moving. All of these many paths are summed to determine the evolution of $|\psi\rangle$, the electronic state. In this paper our focus is not on the state $|\psi\rangle$, but on the many paths that contribute to $|\psi\rangle$. The two pictures are mathematically equivalent: starting from a knowledge of paths one can build the electronic propagator which controls the evolution of $|\psi\rangle$, and conversely $|\psi\rangle$'s evolution may be systematically decomposed into the paths which determine it.

To be clear, we are not discussing the semiclassical paths of an electron's average motion. For instance, in a magnetic field an electron's average position executes well-defined circular loops around the axis of the magnetic field, and one can measure this cyclotron motion. This is not the sort of path we are talking about. Instead we are talking about the infinitely many quantum mechanical paths, tracing many complex trajectories and fully exploring the sample, which sum up to produce the average cyclotron motion.

The paths traced by electrons never begin or end in isolation, since in this event electronic charge would not be conserved, i.e. charge would be generated or destroyed. Instead, the creation or annihilation of an electron is always accompanied by the creation or annihilation of an accompanying hole with opposite charge, and by this mechanism charge is conserved. The two paths of an electron and of its corresponding hole, followed from their origin together to their final disappearance together, form a loop.

It is important to be clear that the loops under discussion here are traced by bare electrons and holes, not by quasiparticles. The requirement to move in loops is an immediate consequence of charge conservation and gauge invariance, and does not require that interactions are weak, the existence of a Fermi liquid, or well-defined quasiparticles. Nor does it not assume any other sort of collective many-body behavior. The loop requirement applies independently of magnetic fields, scattering, and interactions. Analysis focused on electron-hole loops is therefore a very powerful way of understanding the mechanisms responsible for electronic transport.

It is also important to be clear that the loops discussed here move through real space, and occur even when disorder is very strong. Therefore they are not the same loops used in the analysis of Berry phases and topological invariants, which are usually calculated in momentum space and assume a well defined band structure. Moreover the loops discussed here concern the bare electron and hole carriers within a material; the U(1) symmetry which supports them comes from electromagnetism, not from effective interactions that occur in spin liquids and other interacting systems.

Experimental data on a sample's dependence on ex-

ternal magnetic field gives direct access to the areas of the electron and hole loops within the sample. Each loop couples to field via a phase which is proportional to the magnetic flux through the loop, and this phase is equal to the product of the loop area and the magnetic field strength. We neglect the Zeeman term, assuming that only the spin singlet contributes to conduction. Within the phase factor magnetic field has a conjugate relationship to area, with a proportionality constant that is determined by fundamental constants and can not be renormalized. Therefore measurements of a sample's dependence on external magnetic field give information about the area of the loops traced by electrons within the sample. More precisely, the area that one learns about is the sum of the areas of all loops that contribute to the conductance. In a non-interacting system this simplifies to the area of a single loop. The methodology of using magnetic fields to measure loops, which we explain further below, does not assume quasiparticle or Fermi liquid physics. It is a simple consequence of charge conservation. In interacting systems

In this article we apply this methodology focused on electron-hole loops and their areas to electrical conduction. We obtain results about the electron and hole loops responsible for Landau levels, SdH oscillations, WL/WAL, and linear magnetoresistance. Our rigor here is limited only by our omission of the Zeeman effect, which amounts to an assumption that only the spin singlet contributes to conduction. Where this assumption is valid, there is a firm link between experimental observables and loop areas. Details of the material's Hamiltonian, eigenstates, interactions, Fermi surfaces, or disorder do not affect this link, and are discussed very little in this paper. Instead we focus on reasoning about the electron and hole loops that are responsible for conduction, and on drawing conclusions about which physical mechanisms are responsible for producing those loops.

B. What We Can Learn From Loop Areas

Our methodology is to start with the conductance's dependence on external magnetic field, and then Fourier transform with respect to magnetic field. The resulting quantity depends on magnetic field's conjugate quantity, the total area of all loops that contribute to the conductance. We call this quantity the loop area distribution. The final step is to examine the weights of this distribution, i.e. the weight corresponding to a particular value of the total loop area, and allow these weights to inform us about what electrons and holes are doing inside the material.

One reference point for comparison is the Landau levels and SdH oscillations, which are phenomena that do not rely on scattering. The loop area distribution for these effects oscillates periodically with loop area, with a period of oscillation that is determined by the Fermi surface. It has both positive and negative signs. Both

the presence of a particular area scale, and oscillations between negative and positive signs (i.e. ringing), are hallmarks of ballistic conduction.

A second reference point is weak (anti)localization (WL/WAL). Here the loop area distribution has a single sign, and does not show any concentration near any particular area scale (i.e. it is scale-free).^{19,20,24} The weights of the loops responsible for the WL/WAL signal decrease gradually and smoothly with area, and the decay follows a $1/A$ (where A is area) power law up to loop areas which are far larger than that determined by the Fermi surface. The very smooth distribution of loop areas and the very large area scales are caused by stochastic motion of the charge carriers, and are unmistakable hallmarks of scattering-driven (diffusive) conduction.

We next compare the loop area distribution responsible for linear magnetoresistance to that of standard WL/WAL, Landau levels and SdH oscillations. We are making the assumption (explicit throughout this paper) that in the linear resistance materials of interest neither spin triplets nor the Zeeman term affect electronic conduction. This is certainly a reasonable assumption for those topological insulators which manifest linear magnetoresistance.

The theoretical predictions for Landau levels, SdH oscillations, and WL/WAL are all based on 2-D electron gas models with no interactions. Therefore the loop area distribution is that of single electron-hole loops. In principle a linear resistance material may be strongly interacting. In this case the loop area distribution would concern the total area of all loops contributing to conduction, and comparison to non-interacting loop area distributions like those of Landau levels or WL/WAL may be misleading. Fortunately this is not a concern in most topological insulators, which are only weakly interacting.

We find that the loop area distribution corresponding to linear magnetoresistance is very like the loop area distribution of WL/WAL. There are no changes in sign, there is no favored length scale, the area distribution decreases smoothly as area increases, and very large area scales are seen. This is evidence that scattering and stochastic motion are key to linear magnetoresistance. This is also evidence that linear magnetoresistance is caused by Cooperons, i.e. paired particles and holes, rather than by any species of single-particle motion. The phase of single electrons and holes oscillates very rapidly at the Fermi wavelength, which is the ultimate reason why the loop area distribution of Landau levels exhibits an oscillating sign. In contrast the phase of a Cooperon varies at the much longer localization length, resulting in a very smooth single-sign loop area distribution.

Despite these similarities, there is one major difference between WL/WAL and linear magnetoresistance: the latter has a much longer tail than the former; the loop area distribution of linear magnetoresistance decays like $\ln A$ while WL/WAL decays like $1/A$. In other words, linear magnetoresistance has many more large loops, and much larger loops. This reweighting towards large loop

areas is the opposite of what would be obtained by transitioning from 2-D conduction to 3-D conduction. It is impossible to explain if Cooperons move diffusively in 2-D, whether with ordinary random walks, or with Levy flights.

The extraordinarily long and fat tail seen in linear magnetoresistance shares something in common with Landau levels, whose loop area distribution is a simple cosine. In the absence of scattering and at zero temperature, this cosine extends to infinitely large areas, signifying that all sizes of electron-hole loops are in play. The reason is not, of course, that the electrons are exploring an infinite 2-D plane. Instead the repeated oscillations of the loop area distribution signify that if an electron can complete one cyclotron orbit, then it can complete any number of cyclotron orbits. The electron's ability to retrace its path around a loop is a manifestation of quantum coherence. If finite temperature disrupts quantum coherence, its effect is to cut off loops with large areas.

In two dimensional samples the Cooperons that produce WL/WAL do not repeat their loops; they are effectively random walkers moving according to purely classical dynamics, without quantum coherence. The reason is that scattering randomizes momentum, and therefore even when a random-walking Cooperon returns to its starting point, it starts off from there in a new direction. This is a peculiarity of 2-D planar materials. When Cooperons are confined to the 2-D surface of a wire, or move one dimensionally around a circle, then they do manifest quantum coherence and repeat their loops.

Linear magnetoresistance involves much larger loop areas than can be explained via Cooperons undergoing ordinary random walks. We therefore conclude that the Cooperons in linear magnetoresistance materials retain some degree of quantum coherence, allowing them to sometimes repeat their loops. In other words, linear magnetoresistance is caused by a combination of quantum coherence and scattering - a combination that is difficult to account for in planar 2-D materials. Further discussion of this topic is in Section III.

Section I will begin with charge conservation and show that it implies that magnetic field is conjugate to area. This allows one to start with experimental measurements of the conductance's dependence on magnetic field and then obtain information about the areas of electron and hole loops. Next section II applies this methodology to calculate and compare the loop area distributions of Landau levels, SdH oscillations, WL/WAL, linear magnetoresistance, and Levy flights. Section III discusses linear magnetoresistance and possible links to quantum coherence, and section IV wraps up with a few final thoughts. Appendix A discusses several ways of regularizing the Fourier transform from $1/A$ to the logarithm and vice versa, and Appendix B gives some more speculative comments on materials with linear-in-temperature resistance, such as bad metals.

I. GEOMETRIC ANALYSIS OF ELECTRON AND HOLE LOOPS

Charge conservation is a fundamental feature of nature which has been subjected to intense scrutiny and has been found to be obeyed to extreme precision. Two strategies are available to engineer a theory to correspond to this experimental reality. One strategy is to select a set of quantum mechanical states available to the system, and a Hamiltonian which describes the system's ground state and dynamics. In the process of building the states and the Hamiltonian, one enforces a constraint: all states must have the same total charge, and the Hamiltonian may not change that charge. This approach is very powerful, and has shown extreme versatility in building models of the essential physics of many systems. These include simplified models where the electron's position is restricted to an integer number of discrete values and therefore electron paths are series of discrete jumps. However this approach has the weakness that charge conservation is essentially imposed by fiat, and that its fundamental connection to the geometry of electron and hole loops is lost.

To capture the geometry of electrons moving in the real world, it is necessary to start from the symmetries of the real world. These include continuous translation, i.e. the electrons' ability to move smoothly along continuous paths instead of jumping from position to position, and Poincare symmetry, the ability to smoothly change direction in the four dimensional manifold of space and time. The class of theories which unite these symmetries to quantum mechanics, relativistic quantum field theory, is our starting point for understanding the connection between charge conservation and geometry.

An early and essential result of relativistic quantum field theory was the Dirac equation, which predicted the existence of holes. Soon afterwards quantum electrodynamics was formulated, in which the principle of gauge invariance is key to guaranteeing charge conservation. Later the constraints of internal consistency (renormalizability, unitarity, etc.) and of experimental data resulted in the standard model, in which gauge invariance is elevated to a guiding principal that is key to all electronic interactions. The standard model incorporates quantum electrodynamics, and preserves its treatment of charge conservation of electrons and holes, which is based on gauge invariance.

Gauge invariant theories are built in two steps. The first step is adding a gauge field: a $U(1)$ phase $\phi(\vec{x})$ which depends on position. This phase modifies the momentum operator which describes translational motion, so that as an electron moves along its path, its phase is multiplied by the difference between the phases $\exp(i\phi)$ at the electron's final position and its initial position. The second and final step toward building a gauge invariant theory is the requirement that the theory be invariant under arbitrary changes of the gauge field. This is essentially a mathematical shorthand for imposing a restriction on the

structure of every physical observable. The only way to build an observable \mathcal{O} which is independent of $\phi(\vec{x})$ is by requiring each electron contributing to the observable to return to its starting position, forming closed loops. Because the final and initial positions are the same, the difference in phase $\exp(i\phi)$ between start and end is exactly zero, and therefore observables built from closed loops do not depend on $\exp(i\phi)$; they are gauge invariant. The actual shape and size of the loops, and also the number of loops, is completely unrestricted by gauge invariance; the emphasis is on their closed nature.

In relativistic quantum field theory the electron paths move through space-time, and the requirement to return to the origin does not mean only that an electron must reverse its motion in space. Each electron is also required to reverse its direction in time, so it can eventually return to its starting time. From one point of view this reversal of direction is simply a manner of pulling a loop's path back to its origin, but from another point of view the reversal of time-direction is the meeting (creation or annihilation) of a particle-hole pair. In other words, one can adopt a vocabulary that avoids discussing electrons moving backwards-in-time, but only at the cost of saying that for every electron [moving in forward in time] there is also a hole. The hole is thought of as moving forward in time, but it has exactly the same mathematical and physical consequences as an electron moving backward in time. The net effect is that instead of talking about electrons tracing loops in space-time, one requires that electrons and holes are always produced and destroyed in pairs. If one takes the hole and electron paths together one finds that they always add up to loops in space-time. This loop structure is an immediate and unavoidable consequence of combining gauge invariance with special relativity.

Gauge invariance ensures charge conservation in a way that is so powerful that it seems almost trivial, as follows. First it requires that that observables be made out of space-time loops. Secondly we divide up each space-time loop into segments that move forward in time [electrons], and segments that move backward in time [holes]. Thirdly we assign charge $-e$ to electrons and charge $+e$ to holes. Fourthly we note that the loop structure implies that electrons are always created or destroyed with corresponding holes, in pairs. We thus arrive at charge conservation: this structure of pair-wise creation/destruction manifestly conserves total charge.

A. Coupling Magnetic and Electric Fields to Loops

In relativistic quantum field theory the effect of magnetic and electric fields on electrons is mediated by the minimal coupling: the momentum operator p^μ is replaced by $p^\mu - eR^\mu$, where the gauge potential $R^\mu = \partial^\mu \phi$ is the first derivative of the gauge phase $\phi(\vec{x})$. The electric and magnetic fields \vec{E}, \vec{B} are encoded in $R^\mu = (\phi/c, \vec{R})$ via $\vec{E} = -\vec{\nabla}\phi - \partial\vec{R}/\partial t$ and $\vec{B} = \vec{\nabla} \times \vec{R}$. This minimal coupling is required to construct a gauge invariant con-

tinuum theory - it is necessary to ensure that when an electron moves from a starting position to a final position, it is multiplied by the difference in phases $\exp(i\phi)$ at the two positions.

The minimal coupling implies that as an electron or hole traces its path, the only effect of electric and magnetic fields is to introduce a multiplicative factor, the Wilson loop $W_\gamma = \exp(i \oint_\gamma ds_\mu R^\mu)$.^{25,26} The line integral $\oint_\gamma ds_\mu$ is taken along the electron/hole path, denoted by γ . It is a loop integral because electron and hole paths are required to form loops.

When several electron-hole loops occur the line integrals of each loop add up, and the multiplicative factors $\exp(i \oint_\gamma ds_\mu R^\mu)$ multiply each other. Therefore we shift the notation from γ which specifies a single loop to Γ , which specifies the paths traced by a set of one or more electron and hole loops. The total effect of all the loops together is to multiply by $W_\Gamma = \exp(i \oint_\Gamma ds_\mu R^\mu)$, where the line integral $\oint_\Gamma ds_\mu$ is the sum of each of the loop integrals $\oint_\gamma ds_\mu R^\mu$ in Γ , summing over the one or more loops specified by Γ . Gauge invariant observables are built from sums in which each term of the sum has a particular set of electron-hole loops specified by Γ and is weighted by the corresponding Wilson loop W_Γ .

By Stokes' theorem the phase $\oint_\Gamma ds_\mu R^\mu \equiv \Phi_\Gamma$ in the Wilson loop is equal to the electro-magnetic flux through the one or more loops specified by Γ . In other words, the line integral $\oint_\Gamma ds$ over loops Γ is equivalent to a flux integral $\int_\epsilon dS$ over the surfaces ϵ bounded by the loops. Mathematically $\oint_\Gamma ds_\mu R^\mu = \Phi_\Gamma = \int_\epsilon dS_{\mu\nu} F^{\mu\nu}$. Here $F^{\mu\nu} = \partial^\mu R^\nu - \partial^\nu R^\mu$ is the electromagnetic field tensor whose components are equal to the electric and magnetic fields, and $dS_{\mu\nu}$ is the infinitesimal surface tensor for a surface embedded in four-dimensional space-time. When the surfaces ϵ are all fixed to a particular time t this flux simplifies to the magnetic flux $\Phi_\Gamma = \int_\epsilon d\vec{S} \cdot \vec{B}$, where now $d\vec{S}$ is the surface infinitesimal in three-dimensional space and \vec{B} is the magnetic field.

In atomic units where $e = \hbar = 1$ the phase Φ_Γ controlling the Wilson loop $W_\Gamma = \exp(i\Phi_\Gamma)$ is equal to the electromagnetic flux through all the loops specified by Γ . Because both the phase and the flux are strictly the argument of an exponential, they must be unit-free. In turn the units of electromagnetic field $F^{\mu\nu}$ must be the inverse of the units of the area infinitesimal $dS_{\mu\nu}$. This is the fundamental reason why the electromagnetic field tensor $F^{\mu\nu}$, and magnetic field \vec{B} in particular, have units of inverse area.

We formalize these ideas using the loop representation of observables.²⁷ The previous discussion can be summarized by the statement that every physical observable $\mathcal{O}_i(\vec{B})$ must be written as

$$\mathcal{O}_i(\vec{B}) = \sum_\Gamma \langle \mathcal{O}_i | \Gamma \rangle \exp(i\Phi_\Gamma) \quad (1)$$

where Γ specifies the spatial trajectories of all the electron-hole loops, and \sum_Γ is a sum over all the ways

these electron-hole loops can be arranged - i.e. both their number and their individual trajectories. \mathcal{O}_i is the observable, and $\langle \mathcal{O}_i | \Gamma \rangle$ is the weight with which a particular Wilson loop Γ contributes to \mathcal{O}_i . This weight is determined by both the observable and by the kinetics and interactions of the electrons and holes tracing the loops specified by Γ .

B. The non-relativistic limit

In relativistic quantum field theory the electron-hole pair follows a path which curves through space time and finally returns to its origin. The energy of the electron and the energy of the hole, taken separately, vary throughout their motion around the loop.

The non-relativistic limit is taken by assuming that the energies of the electron and hole are almost constant and remain very near their rest energy/mass. Obviously this requires a strict conceptual division between electron and hole. In this limit the Dirac equation, describing both electron and hole, simplifies to the Pauli equation which describes either the electron or the hole.

Because of the non-relativistic limit's special treatment of the time dimension, electric field drops out of the minimal coupling and takes a separate role in the Pauli equation, and is joined by the $e\vec{\sigma} \cdot \vec{B}$ Zeeman term. The remaining minimal coupling is $\vec{p} - e\vec{R}$, where \vec{R} is the gauge field determining the magnetic field by $\vec{B} = \vec{\nabla} \times \vec{R}$. The minimal coupling produces Wilson loops $\exp(i\Phi_\Gamma)$ where the flux $\Phi_\Gamma = \int_\epsilon d\vec{S} \cdot \vec{B}$ depends only on magnetic field not electric field.

In the non-relativistic limit magnetic field affects electronic motion not only through Wilson loops but also via the Zeeman term. As we have argued earlier, in a class of systems which includes topological insulators in the diffusive regime, the spin triplet relaxation time τ_t is short compared to the spin singlet relaxation time τ_s . Therefore spin and the Zeeman term do not contribute to electronic transport over long distances²², and observables measuring transport depend on magnetic field only via Wilson loops, not via the Zeeman term.

C. External Fields and the Loop Area Distribution

We specialize to the case of a uniform magnetic field \vec{H} originating externally to the sample, which we will call $\vec{B}^{ext} \equiv \vec{H}$. We consider the effect of \vec{B}^{ext} on the one or more electron-hole loops specified by Γ . Each electron-hole loop experiences not only the external field \vec{B}^{ext} , but also magnetic field generated by the electron-hole loops within the sample. The total field, including both external field and the field generated by the sample, is called \vec{B} . Total field \vec{B} is related to external field \vec{B}^{ext} via $\vec{B} = \mu_0 \vec{B}^{ext} + \mu_0 \vec{M}$, where \vec{M} is the magnetization. μ_0 is the vacuum permeability, which we will drop for

simplicity. In diamagnetic materials, including superconductors, \vec{B} is smaller than \vec{B}^{ext} , while in paramagnetic materials \vec{B} is larger than \vec{B}^{ext} . We separate the magnetic flux through a Wilson loop into two terms: a flux Φ_{Γ}^{int} caused by the field generated by the sample, and a flux $\Phi_{\Gamma}^{ext} = \int_{\epsilon} d\vec{S} \cdot \vec{B}^{ext}$ from external field. Therefore in an external magnetic field observables can be written as

$$\mathcal{O}_i(\vec{B}^{ext}) = \sum_{\Gamma} \langle \mathcal{O}_i | \Gamma \rangle \exp(i\Phi_{\Gamma}^{ext}) \quad (2)$$

The phase Φ_{Γ}^{int} from field generated within the sample is now packaged inside the weight $\langle \mathcal{O}_i | \Gamma \rangle$. The phase $\exp(i\Phi_{\Gamma}^{ext})$ depends only on external field, not on internally-generated field as well.

Because the external field \vec{B}^{ext} has uniform direction and magnitude, it is useful to assign to each Wilson loop a vector-valued cross-section $\vec{A}_{\Gamma} = \int_{\epsilon} d\vec{S}$, which is a vector generalization of the Wilson loop's surface area. This area vector depends only on paths traced by the loop Γ , not on the shape of the surfaces ϵ which are bordered by Γ . The magnetic flux through Γ then simplifies to the dot product of the area \vec{A} with the external field \vec{B}^{ext} ; $\Phi_{\Gamma} = \vec{A}_{\Gamma} \cdot \vec{B}^{ext}$. This leads to our central result:

$$\begin{aligned} \mathcal{O}_i(\vec{B}^{ext}) &= \int d\vec{A} \mathcal{O}_i(\vec{A}) \exp(i\vec{A} \cdot \vec{B}^{ext}), \\ \mathcal{O}_i(\vec{A}) &\equiv \sum_{\Gamma} \langle \mathcal{O}_i | \Gamma \rangle \delta(\vec{A}_{\Gamma} - \vec{A}) \end{aligned} \quad (3)$$

In other words, every physical observable can be resolved into contributions corresponding to specific areas \vec{A} , each with weight $\mathcal{O}_i(\vec{A})$:

$$\mathcal{O}_i(\vec{A}) = \int \frac{d\vec{B}^{ext}}{(2\pi)^3} \mathcal{O}_i(\vec{B}^{ext}) \exp(-i\vec{A} \cdot \vec{B}^{ext}) \quad (4)$$

The area \vec{A} is the sum of the areas of all the electron-hole loops that contribute to the observable.

In summary, equations 3 and 4 state that measurements of an observable $\mathcal{O}_i(\vec{B}^{ext})$'s dependence on external magnetic field give direct and rigorous information about the sum of the areas traced out by electron loops within a sample, simply by performing a Fourier transform. The resulting loop area distribution $\mathcal{O}_i(\vec{A})$ completely describes how different loop areas contribute.

From a theorist's point of view, the problem of how to perform a regularized sum over loops \sum_{Γ} , i.e. how to control both long distance and short distance contributions to the sum, remains in general unsolved. This makes evaluation of the sum over loops \sum_{Γ} in equations 1 and 3 a difficult task. It is therefore both remarkable and encouraging that we can measure the sum experimentally and directly using equation 4; experimental measurements of the loop area distribution $\mathcal{O}_i(\vec{A})$ can lead the way in guiding theorists to correct procedures for performing the sum over loops.

II. COMPARISON OF LOOP AREA DISTRIBUTIONS

Throughout the remainder of this paper $\vec{B} = \vec{B}^{ext} = \mu_0 \vec{H}$ means the external magnetic field, and $B = |\vec{B}|$ is its magnitude.

A. Landau levels and SdH Oscillations

To illustrate the transformation from the magnetoconductance to the loop area distribution, consider the case where the dominant energy scale is the Fermi level E_F , in which case a delta function - the first Landau level - will be found in $G_{xx}(B)$ at $B^{-1} = \frac{1}{2}A_F$. Here $2\pi/A_F \propto 2\pi E_F$ is the cross-section of the Fermi surface.²⁸ The loop area distribution is therefore a cosine $G_{xx}(A) \propto \cos(A/\frac{1}{2}A_F)$, which means that loops with every area contribute to the conductance and that there is ringing corresponding to the characteristic Fermi area A_F .⁷⁷

The most interesting aspect of this result is that quantum coherence causes the first Landau level to be repeated exactly at characteristic areas $(N + 1/2)A_F$, with the N -th level's height proportional to N . The repetitions are manifested as a hierarchy of additional Landau level delta functions in $G_{xx}(B)$, as illustrated in Figure 1a. Figure 1b shows the loop area distributions $G_{xx}(A)$ of the Landau levels. The N -th Landau level is a cosine $\cos(A/(N + \frac{1}{2})A_F)$ with period equal to $(N + 1/2) 2\pi$ times the characteristic area A_F . In mathematical terminology, the N -th Landau level is simply the N -th harmonic of the lowest Landau level. Speaking more plainly, quantum coherence ensures that if an electron can complete a loop once, then it can repeat that same loop any number of times.

The only limit to these repetitions (harmonics) is decoherence caused either by the scattering energy scale Γ or by the temperature T , which causes a decay in the loop area distribution.²⁹ Decoherence broadens the Landau levels into peaks with width Γ, T , which eventually merge into SdH oscillations. These oscillations have equal height instead of the height proportional to N seen in Landau levels. They decay exponentially when the value of $B = N^{-1}A_F^{-1}$ descends to Γ, T , and their loop area distribution also decays exponentially at areas larger than Γ^{-1}, T^{-1} .^{29,78}

B. Weak Antilocalization

We now investigate 2-D WL/WAL, whose magnetoconductance $G_{xx}^{WAL}(B)$ has been studied extensively. We will show that the WL/WAL loop area distribution varies inversely with area i.e. it obeys $G_{xx}^{WAL}(A) \propto A^{-1}$. At magnetic fields less than the inverse cutoff $q_C B < 1/L_{max}^2$ the conductance $G_{xx}^{WAL}(B)$ is controlled by the cutoff: it quickly transitions to zero, and this transition

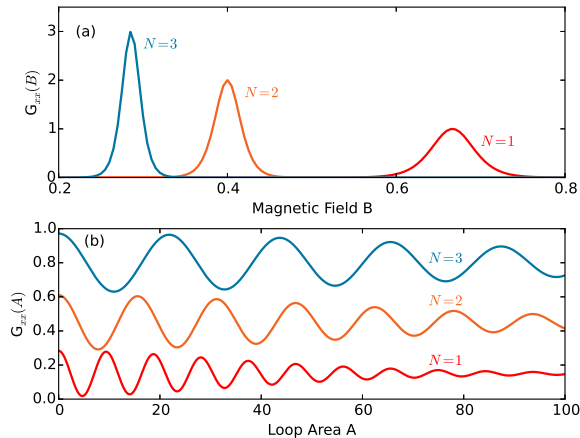


FIG. 1: (Color online.) Quantum coherence and the hierarchy of Landau levels. Panel (a) shows the magnetoconductance $G_{xx}(B)$ of the $N = 1, 2, 3$ Landau levels and panel (b) shows their loop area distributions $G_{xx}(A)$, which have been vertically shifted for clarity.²⁹ Quantum coherence is responsible for producing higher harmonics of the lowest Landau level, causing higher Landau levels at multiples $(N + \frac{1}{2})A_F$ of the characteristic area $A_F = E_F^{-1}$. Decoherence, i.e. loss of quantum coherence, is caused by either the scattering energy scale Γ or the temperature T . Decoherence widens peaks in $G_{xx}(B)$, suppresses $G_{xx}(A)$ at large A , and completely suppresses oscillations when the field B is as small as Γ, T . $E_F = 1$, $\Gamma = 0$, $T = 0.05$.

is quadratic in B because time reversal symmetry requires that G_{xx} be even under $B \rightarrow -B$. At larger fields $q_C B > 1/L_{max}^2$ the magnetoconductance of a 2-D spin singlet is a logarithm $G_{xx}^{WAL}(B) \propto -\ln B$. This logarithmic form, which will be our focus here, is robust and ubiquitous. If spin or orbital degrees of freedom are in play then the logarithmic conductance seen from the Cooperon spin singlet generalizes simply to a sum of logarithms corresponding to the Cooperon spin singlet, the Cooperon spin triplet, and possibly other Cooperon sectors associated with valley degrees of freedom etc. The logarithmic conductance is seen for both Dirac and $p^2/2m$ dispersions, for both lattice and continuum models, for both short and long range scattering, and for a wide variety of quasi-2-D geometries.^{20,30–42,79} The logarithm is found in all 2-D systems that are in the diffusive regime, i.e. all 2-D systems whose size is larger than the momentum relaxation length caused by scattering.

The reason that the same form of $G_{xx}^{WAL}(B)$ is universally found in diffusive 2-D systems is that at distances exceeding the momentum relaxation length the Cooperon loses all information about momentum and kinetics, and therefore its trajectory is simply a 2-D random walk. When spin or orbital degrees of freedom are in play the Cooperon carries several species of random walkers (e.g. a spin singlet and a spin triplet), but each of the species

is still performing a simple random walk. The WL/WAL magnetoconductance signal is determined by Cooperon trajectories which return to their origin, forming loops. Quantum coherent repeats of loops do not contribute because the Cooperon's momentum is random and therefore even when a Cooperon returns to its origin it does not have the same momentum that it started with. Since the trajectories of these Cooperon loops are simply random walks, the magnetoconductance signal has the same form in all 2-D diffusive systems.

The fact that the universal form of the magnetoconductance $G_{xx}^{WAL}(B) \propto \ln B$ is logarithmic was first determined by Ref.²⁰. Ref.²⁰ starts with a description of how scattering changes the motion of the electronic wavefunction $|\psi\rangle$ and its complex conjugate $\langle\psi|$, and then uses this information to derive the behavior of the Cooperon, which is a pairing of $|\psi\rangle$ with $\langle\psi|$. It is found that the spin singlet component of the Cooperon is simply a random walker and that every random walk returning to the origin contributes with equal weight to the WAL conductance $G_{xx}^{WAL}(B)$. Mathematically this is expressed by writing the Cooperon Green's function as the inverse of a Laplacian operator which expresses how individual steps in the walk are taken. To derive from disordered scattering the Cooperon and its random walk, Ref.²⁰ uses the standard field theory of disordered scattering, bosonization, and sigma models.^{18,19} In this respect it is generally imitated by all other theoretical (non-computational) treatments of Cooperons and WL/WAL. Always the result is that WL/WAL is mediated by random walking Cooperons.

The WAL conductance is proportional to the probability that the Cooperon will return to its origin; mathematically it is the diagonal $\vec{x} = \vec{x}$ matrix element of the Cooperon Green's function. At zero field $G_{xx}^{WAL}(B=0)$ is simply the probability that random walkers will return to their origin, while non-zero field causes each walker trajectory to be reweighted by a Wilson loop phase factor. Calculation of the Cooperon spin triplet component is almost identical to that of the singlet - the main difference is that the triplet contribution to G_{xx} is multiplied by -1 , producing weak localization instead of weak antilocalization.

We emphasize the fact established in Ref.²⁰ that all trajectories contributing to the Cooperon's spin singlet component contribute with the same weight, with no phase factor from kinetics, scattering, potentials, or time evolution. Likewise, all trajectories contributing to the Cooperon's triplet component contribute with the same weight. In other words, although the Cooperon describes a special kind of quantum interference process that is exhibited by electrons, the actual behavior of a Cooperon is no different than that of a purely classical random walker. No phase information enters in because a Cooperon is a pairing of $|\psi\rangle$ with $\langle\psi|$, and their phases cancel each other. Therefore the Cooperon evolves as a classical random walker, and calculations of $G_{xx}^{WAL}(B)$ look purely classical. All Cooperon trajectories (of the singlet, or

of the triplet) contribute with the same sign and weight. One very important consequence is that the loop area distribution $G_{xx}^{WAL}(A)$ of the Cooperon singlet (or triplet) trajectories has only one sign, like a purely classical probability distribution. Calculation of WL/WAL is isomorphic to calculating return probabilities of a purely classical walker.

This picture of a purely classical Cooperon is modified in samples with sizes approaching the localization length, where the conductance is reduced to the order of the universal conductance quantum G_0 . At this long length scale processes coupling two or more Cooperons become important, as do processes coupling Cooperons with diffusons. However the systems which show the *weak* localization and antilocalization which is our focus here lie far from the localized limit, so that the WL/WAL contribution remains at the level of simple random walks without multi-Cooperon processes.

We demonstrate here that the Fourier transform of the logarithmic WL/WAL conductance $G_{xx}(B) \propto \ln B$ varies inversely with area, i.e. that the loop area distribution obeys $G_{xx}(A) \propto A^{-1}$. In other words the Fourier transform of $-\ln B$ is A^{-1} and, vice versa, the inverse Fourier transform of A^{-1} is $-\ln B$. The main difficulty is controlling the ultraviolet and infrared cutoffs, so we perform the demonstration three ways. First, we use purely dimensional analysis: $G_{xx}(A) = (2\pi)^{-1} \int dB \exp(-iAB) \ln B$. Therefore $G_{xx}(A)$ must carry units of inverse area; it must be equal to A^{-1} times some function that depends only on dimensionless quantities.

Second, we use specific functional forms for $G_{xx}(A)$ and carry out analytically the inverse Fourier transform from $G_{xx}(A)$ to $G_{xx}(B)$. For instance, we consider hard cutoffs at A_0 and A_{max} , with $G_{xx}^{WAL}(A) = A^{-1}$ for $A_0 < A < A_{max}$. With these cutoffs we arrive at $G_{xx}^{WAL}(B) \approx R_0 - \ln |q_C B| + (q_C B A_0)^2 / 4$ for $1/A_{max} < q_C B < 1/A_0$, where q_C is the Cooperon charge, $R_0 = -\gamma_E - \ln |A_0|$, and γ_E is the Euler-Mascheroni constant. Here R_0 should be adjusted to zero, as a regularization compensating for the hard cutoffs, to replicate the well-known fact that the WAL (Cooperon spin singlet) contribution to the conductance is always positive for all values of B , and that the triplet WL contribution is always negative.²⁰ The appendix imposes several other cutoffs on $G_{xx}^{WAL}(A) = A^{-1}$, in each case performs the Fourier transform exactly, and in each case obtains logarithmic forms for $G_{xx}^{WAL}(B) = \int dA \exp(iAB) A^{-1} \propto -\ln B$.

Lastly, Ref.²⁰ and many subsequent works have established that the magnetoconductance $G_{xx}^{WAL}(B)$ of a 2-D random walking Cooperon is logarithmic. Therefore we can show that the Fourier transform of $-\ln B$ is A^{-1} simply by showing that the loop area distribution of 2-D random walkers is $G_{xx}^{WAL}(A) \propto A^{-1}$. The reasoning is like a syllogism: random walkers have a logarithmic magnetoconductance, and random walkers have an A^{-1} loop area distribution. The loop area distribution is the Fourier transform of the magnetoconductance; therefore

the Fourier transform of $-\ln B$ is A^{-1} .

Figure 2a summarizes the results of extensive numerical Monte Carlo simulations of random walks, all of which verify that the loop area distribution of random walks which return to their origin scales with A^{-1} . We use an infinite 2-D square lattice, and define the lattice spacing equal to one. The walkers take steps which are chosen from a Gaussian distribution with mean step length $l = 4\sqrt{2}, 8\sqrt{2}$, and an upper bound (IR cutoff) to the loop areas is supplied by limiting the walk length to 5×10^5 . We count the walkers which return to their origin, compute the area of the loop traversed by each walker, and histogram the area distribution $G_{xx}(A)$. Panel (a) shows $G_{xx}(A)$, multiplied by A . The plateaus of constant $G_{xx}(A) \times A$ extending over several orders of magnitude verify that 2-D random walks follow an A^{-1} loop area distribution. We have verified that similar results are found with other cutoffs and with other probability distributions governing the step lengths, and a similar numerical Monte Carlo simulation of 2-D random walks has previously verified the A^{-1} loop area distribution.⁴³ These numerical demonstrations of the A^{-1} loop area law again verify that the Fourier transform of $-\ln B$ is $G_{xx}(A) \propto A^{-1}$, and vice versa.

C. Linear magnetoresistance

This result can be reversed and applied to the case of linear magnetoresistance, where $G_{xx}(B) \propto B^{-1}$. We established above that the inverse Fourier transform of A^{-1} is $-\ln B$; interchanging A with B shows that the loop area distribution corresponding to linear magnetoresistance is logarithmic, $G_{xx}(A) \propto -\ln A$. This profile, whose broad features are general for any roughly linear resistance, is remarkably different from the A^{-1} distribution that governs loops generated by random walks. It has fewer small loops and many more large loops; a small head and a very long tail. We emphasize that the logarithmic loop area distribution is a rigorous result, as long as only spin singlets contribute to conduction and the Zeeman effect can be neglected. If this assumption holds, then linear magnetoresistance implies a logarithmic loop area distribution, no matter what physical mechanism is responsible for producing the loops.

D. Levy Flights and 3-D

Since linear magnetoresistance corresponds to a $\ln A$ distribution that decays very slowly with loop area, it would be of interest to determine how such a long tail can be produced. However the $1/A$ decay seen in WL/WAL seems to be the slowest decay and the biggest tail that can be produced by purely stochastic random walks moving on a 2-D lattice. Figure 2b shows the loop distribution that is obtained if the Cooperon does not follow a diffusive path where the step length distribution has a

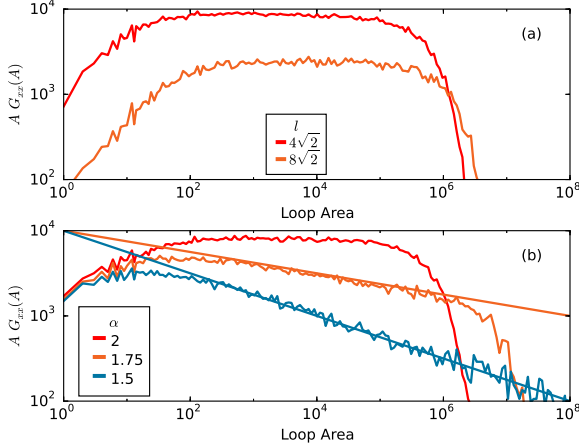


FIG. 2: (Color online.) The Cooperon's loop area distribution $G_{xx}(A)$ obtained by Monte Carlo simulations. Panel (a) shows $G_{xx}(A)$, multiplied by A , of standard 2-D random walks with Gaussian-distributed steps having average length $l = 4\sqrt{2}, 8\sqrt{2}$. The plateaus extending over several orders of magnitude verify that 2-D random walks follow an A^{-1} loop area distribution. The IR cutoff is caused by limiting the walk length to 5×10^5 . Panel (b) shows that Levy flights have a loop area distribution which decays faster than A^{-1} . α is the stability parameter of the Levy alpha-stable distribution which controls the step lengths. $\alpha = 2$ produces Gaussian-distributed steps, and when α is decreased below 2 the distribution develops a heavy tail of very long steps. The straight lines are for $10^4 \times A^{-0.125}$ and $10^4 \times A^{-0.25}$, and their agreement with the Monte Carlo data shows that $G_{xx}(A) \propto A^{-2+\alpha/2}$. $l = 4\sqrt{2}$ and the IR cutoff is 5×10^5 , 1.5×10^6 , and 5×10^6 for the $\alpha = 2, 1.75, 1.5$ results.

finite mean, variance, etc. Instead the Cooperon in Figure 2b follows a Levy flight where step lengths follow a distribution including both short and very long steps. The result is a steeper decay than A^{-1} , because long steps tend to decrease the probability that the walker's path will complete a loop. Here we again use a 2-D square lattice, choose random steps from a probability distribution, and impose an IR cutoff l on the maximum path length. The only difference from Figure 2a is that instead of choosing steps from a Gaussian probability distribution to produce a random walk, we choose steps from the Levy alpha-stable distribution, producing Levy flights where most steps are short but some steps are very long. The Levy alpha-stable distribution is controlled by the Levy distribution stability parameter α which we give values $\alpha = 2, 1.75, 1.5$. When $\alpha = 2$ it reduces to the Gaussian distribution, and when α is decreased below 2 the distribution develops a fat tail of very long steps. Panel 2b plots $G_{xx}(A) \times A$. At $\alpha = 2$ we see again the plateau signaling the $1/A$ area decay law of random walks. At $\alpha = 1.75, 1.5$ the loop area distribution decays faster than A^{-1} , tilting the plateau. We superimpose straight lines for $10^4 \times A^{-0.125}$ and $10^4 \times A^{-0.25}$, and their agreement with the $\alpha = 1.75, 1.5$ Monte Carlo

data shows that $G_{xx}(A) \propto A^{-2+\alpha/2}$. In summary, Levy flights steepen the area law decay, taking it further from the very slow $\ln A$ decay necessary to produce linear magnetoresistance.

Increasing the dimensionality above two dimensions also produces a steeper decay, $A^{-3/2}$ in 3-D.⁴⁴ This is the opposite of what is wanted, so one might like to instead decrease the dimensionality below two dimensions. However in one dimension all loops have area identically equal to zero. Therefore neither changing the step distribution nor changing the dimensionality can reproduce the $\ln A$ tail seen in linear magnetoresistance systems.

We note that in very strong magnetic fields where the magnetic length $l_H = \sqrt{\hbar c/eB}$ is smaller than the mean free path a \sqrt{A} area law is obtained at areas smaller than l_H^2 .^{45–48} However this produces a $1/\sqrt{B}$ magnetoresistance, not a linear signal, and is strictly a large-field behavior, unlike experiments where linear magnetoresistance starts at small fields.

III. LINEAR MAGNETORESISTANCE AND QUANTUM COHERENCE

Linear magnetoresistance's $-\ln A$ loop area distribution shows no characteristic scale, decreases uniformly and smoothly, and never changes sign. These facts are strong evidence that linear magnetoresistance is caused by Cooperons, i.e. by paired particles and holes scattering together, rather than by any species of single-particle motion.

The loop area distribution of linear magnetoresistance exhibits a long fat logarithmic tail that can not be explained by random walks or by Levy flights. Therefore we propose that the Cooperons responsible for linear magnetoresistance do follow random walks, but with the special feature that they maintain quantum coherence, allowing them to repeat their loops many times, in the same way that Landau levels are repeated in a hierarchy at $(N + \frac{1}{2})A_F$.

As a simple example, consider the case of 2-D random walks with hard cutoffs at A_0 and A_{max} and $G_{xx}^1(B, A_0, A_{max}) = \int_{A_0}^{A_{max}} dA \cos(q_C B A)/A$. The $1/A$ in this expression is the loop area distribution of standard random walks, and the cosine and integral perform the Fourier transformation from area to magnetic field. q_C is the Cooperon charge. At field strengths between the UV cutoff $1/A_0$ and the IR cutoff $1/A_{max}$ this magnetoconductance $G_{xx}^1(B, A_0, A_{max})$ follows the logarithmic form of standard WL/WAL.

Now take that expression, and allow loops to repeat up to N times, with a weight proportional to $1/N$. This procedure depletes the loop distribution's head, because if a loop area distribution has a UV cutoff at A_0 , then its $N = 2$ first repetition will have a higher UV cutoff at $2A_0$, its second repetition will have its cutoff at $3A_0$, etc. Therefore between A_0 and $2A_0$ the total loop area distribution will have a contribution from only the base

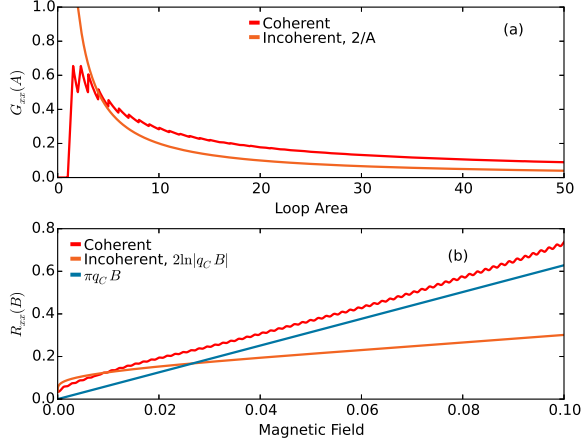


FIG. 3: (Color online.) Linear magnetoresistance from quantum coherence. The red lines show the results when quantum coherence allows loops to repeat up to $N = 100$ times. They can be compared to the orange lines which show standard behavior without quantum coherence. Panel (a) shows the loop area distribution $G_{xx}(A)$, where the quantum coherent distribution (red line) clearly has a small head and long tail as compared to the standard distribution (orange line). Panel (b) shows the resistance $R_{xx}(B)$. The quantum coherent result (red line) compares nicely to the blue straight line with slope πq_C . $A_0 = 1$, and the sharpness of the hard IR cutoff at $A_{max} = 2000$ causes the ripple in the quantum coherent result. The orange line gives a standard logarithmic curve, $R_{xx}(B) = (0.1 - 2 \ln |q_C B|)^{-1}$.

$N = 1$ loop distribution, while at larger areas higher and higher N will contribute. The net effect is to enlarge the tail of the loop area distribution and shrink its head.

Performing the sum over loop repetitions obtains $G_{xx}(B) = \gamma_E + \sum_{n=1}^N n^{-1} G_{xx}^1(B, nA_0, A_{max})$. We have added a regularization constant γ_E to compensate for cutoff effects. Figure 3a compares this loop area distribution to the diffusive $1/A$ profile produced by random walks without coherence. The new loop area distribution has the required small head and long tail; it is a logarithm. Figure 3b shows its Fourier transform, the magnetoresistance. It is linear, i.e. proportional to $R_{xx}(B) - R_{xx}(B = 0) \approx \pi q_C B A_0$, in the range $1/A_{max} < q_C B < 0.2/A_0$.

This simple example is a proof of principle about how to obtain linear magnetoresistance. We chose an abrupt IR cutoff at A_{max} and an abrupt UV cutoff at A_0 , but the true forms of these cutoffs will be material dependent. These cutoffs can have visible effects. In Fig. 3b superimposed on the linear signal one sees a small amplitude fast ripple, which is ringing caused by the abrupt IR cutoff. A similar ripple has been seen in Ref.¹, signaling that a sharp IR cutoff was present in that experiment. However in most experimental data on linear resistance a ripple is not visible, indicating either a smooth IR cutoff or that magnetic field was not sampled at fine enough

resolution. At large fields the form of the UV cutoff also manifests in the signal's behavior. Our sharp UV cutoff causes strong ringing at large fields $q_C B > 0.2/A_0$ [not shown in Fig. 3b] which overwhelms the linear magnetoresistance signal, but with a suitably chosen UV cutoff the linear growth will extend to larger B .

We note that linear magnetoresistance does not require the IR cutoff A_{max} , i.e. the area scale where phase coherence is suppressed, to be very large. For instance, a coherence area of $(100 \text{ \AA})^2$ would allow linear magnetoresistance to extend down to $\approx 0.3T$. Moreover, scatterers within a sample must not fluctuate or move more quickly than the time required for a Cooperon to complete its loop. However this time scale is extremely short. Using $T^{-1} = 4A$ from Appendix B and $\tau = \hbar/k_B T$, we find that τ is three picoseconds for loops of area $A = (100 \text{ \AA})^2$.

We emphasize that a power law area distribution can always be given a depleted head and long tail by invoking quantum coherence and allowing loop repetitions. The form of the UV and IR cutoffs, the relative weight of each repetition, and even the base loop area distribution $G_{xx}^1(A)$ may be specific to the scattering source and to the mechanism responsible for Cooperon coherence. There are only two fundamental requirements: a scattering process producing an area distribution with broad support across a range of areas, and quantum coherence allowing Cooperon loops to repeat in a hierarchy like that of Landau levels.

The real difficulty here is that ordinarily Cooperons in 2-D planar materials do not display loop repetitions; they do not retrace their path two or more times. The fundamental reason is that in 2-D (or 3-D, 4-D, etc.) when a Cooperon returns to its starting point it does so with a momentum that is different from its original momentum. Therefore on the second time around the Cooperon leaves the origin moving in a direction that is different from its first time around. We now turn to the question of how 2-D Cooperons could retain a degree of quantum coherence.

There are two exceptional cases which prove that under the right circumstances Cooperons are able to maintain quantum coherence; they are able to show quantum loop repetitions similar to the higher harmonics seen in Landau levels and SdH oscillations. The most notable exception is 1-D systems with static disorder. In 1-D the Cooperon's particle and hole are constrained to follow the same path, and the static disorder means that their energies never change, and neither does the magnitude of their momenta. Therefore when a Cooperon returns to its starting point it can easily repeat the same exact loop that it has just ended, starting with a momentum that has the same magnitude and direction as before. As a result Cooperon-mediated quantum interference dominates the behavior of 1-D and quasi 1-D systems: once the system's length L increases enough so that the usual classical $1/L$ Ohm's law decay brings the conductance down to one conductance quantum G_0 , quantum interference takes over. This can take two forms. In most systems

the conductance decay transitions from the $1/L$ Ohm's law to the exponential decay characteristic of Anderson localization.^{49–51} However in topologically protected systems the conductance plateaus at a constant value of G_0 , manifesting a perfectly conducting channel. Both cases manifest complete dominance of quantum interference over classical conduction processes, and are fueled by Cooperons maintaining quantum coherence.^{52,53}

A second case where Cooperons retain quantum coherence is 2-D cylindrical geometries when a magnetic field is parallel to the cylinder. In this geometry the Cooperon produces Altshuler-Aronov-Spivak oscillations where the conductance oscillates as field strength is varied. Without Cooperon loop repetitions, i.e. without quantum coherence, the oscillations would have a simple cosine profile. With the loop repetitions the Altshuler-Aronov-Spivak oscillations deviate strongly from a simple cosine signal.^{54,55}

These two examples prove that the absence or presence of quantum coherence in Cooperons is determined by geometry. In 1-D systems and in 2-D cylindrical systems Cooperons can display loop repetitions. The remaining question is how Cooperon coherence and loop repetitions are preserved in the experiments that report linear magnetoresistance, which generally have non-cylindrical (simply connected) 3-D or 2-D geometries. The cause cannot be a non-Gaussian disorder distribution with large outliers, because non-Gaussian disorder penalizes higher-order processes with small weights.

We speculate, very briefly, that the resolution to this question is in geometry. It may be that in linear resistance materials transport may be locally one-dimensional, with carriers constrained along certain race-track like trajectories. This is seen in snake states in graphene, in edge states in the quantum Hall effect and in topological insulators, and might also be realized in C_4 symmetry-broken (nematic) states in underdoped cuprates.^{56–60} When particle motion is locked to a locally one dimensional track, at any particular point the momentum is limited to only two values differing only in sign, and therefore the Cooperon's position and momentum are locked to each other, up to the same sign. This could allow Cooperons to retain some degree of quantum coherence and result in linear magnetoresistance.

The point of introducing quantum coherence into this discussion was the hope that it could explain the extraordinarily large areas that occur in the loop area distribution of materials whose resistance is linear in field. We close by discussing two other alternatives. First, if spin physics and the Zeeman term were to affect conduction, then the Fourier transform of the magnetoconductance, i.e. the quantity which we call the loop area distribution, will contain information not only about loop areas but also about spin physics. In this case the long tail of the Fourier transform may not say anything about loops but may instead be caused by some spin effect.

In topological insulators the only way that spin physics can affect conduction is if conduction is ballistic instead

of diffusive; if scattering is weak enough or the sample small enough that an electron can transverse the sample with very few scatterings. It is a relatively simple matter for experimentalists to determine whether their sample is diffusive or ballistic. Moreover, the conductance in a ballistic sample would exhibit strong dependence on the geometry, leads, and Fermi energy, and could be expected to oscillate with field. There should be little doubt about whether a particular topological insulator sample is in the diffusive regime. In turn there should be little doubt about the validity of the loop area transform and its long tail.

Second, the area detected in the loop area distribution is the sum of the areas of all loops that contribute to the material's conductance. In non-interacting materials this sum includes only one loop. We found that in the diffusive regime random walkers completing a single loop cannot reproduce the area distribution's logarithmic tail, which motivated our discussion of quantum coherence. However in strongly interacting materials, where a sea of electron-hole loops determine the conductance, the story may run differently. In this case the logarithmic distribution's fat tail and depleted head could be caused by some multi-body effect and not by quantum coherence.

Most topological insulators, including the ones reported to exhibit linear magnetoresistance, are known to be weakly interacting.^{1–4} Therefore it seems unlikely that the long tail of their loop area distribution could be caused by interactions, and we are left again with the same conundrum that led us to quantum coherence.

IV. FINAL COMMENTS

In our view one of the most important aspects of the present work is its methodology, which focuses on geometric analysis of electron and hole loops, and especially on the loop area distribution that can be obtained from Fourier transforms of magnetoconductance data. We have presented a non-perturbative framework for understanding electron and hole behavior that can give additional physical insight. This framework depends only on the assumption that neither the spin triplet nor the Zeeman term affect conduction, which is valid in topological insulators in the diffusive regime, and perhaps in other materials as well. We anticipate experiments focusing on the loop area distribution, with special attention to accessing large areas using carefully controlled small increments of the field, to removing leads effects, and to performing careful Fourier transforms. We also expect increased use of vector magnets and multi-dimensional Fourier transforms.

Appendix A: Alternate Regularizations

We demonstrate in this appendix that reasonable regularizations of the Fourier transform of x^{-1} produce a

logarithm, and vice versa. In our first example we perform the Fourier transform of x^{-1} .

$$\begin{aligned}\mathcal{A}(\gamma, x_0, k) &= \int_0^\infty dx \cos(kx) \exp(-\gamma x) \frac{1}{x + x_0} \\ &= \text{Re}(\exp(x_0(\gamma + ik)) \Gamma(0, x_0(\gamma + ik)))\end{aligned}\quad (\text{A1})$$

$\mathcal{A}(\gamma = 0, x_0 = 1, k)$ is approximately logarithmic in the range $x = [0, 0.1] \times 2\pi$, as can be verified by plotting $\mathcal{A}(\gamma = 0, x_0 = 1, k)/\log(k)$.

Our second example again performs the Fourier transform of x^{-1} , but with a different UV cutoff.

$$\mathcal{B}(\gamma, x_0, k) = \int_0^\infty dx \cos(kx) \exp(-\gamma x) \frac{1}{\sqrt{1 + x^2/x_0^2}} \quad (\text{A2})$$

$\mathcal{B}(\gamma, x_0, k)$ can be integrated exactly, and includes Bessel, logarithmic, Struve, and hypergeometric functions. $\mathcal{B}(\gamma = 0, x_0 = 1, k)$ is approximately logarithmic in the range $x = [0, 0.1] \times 2\pi$.

Our third example performs the Fourier transform of $\log|x|$.

$$\mathcal{C}(\gamma, x_0, k, \nu) = \int_0^\infty dx \cos(kx) \exp(-\gamma x) \log|1 + (x/x_0)^\nu| \quad (\text{A3})$$

This integral can be performed analytically for many values of $\nu = 1, 3/2, 5/3, 7/4, 19/10, 2$, and is always proportional to k^{-1} plus corrections of order k at small k in the range $[0, 0.2]$. For $\nu = 3/2, 5/3, 7/4, 19/10$ it is written in terms of Meijer functions. The value of $k \times \mathcal{C}(\gamma = 0, x_0 = 1, k, \nu)$ at $k = 0$ is generally a rational fraction times π . For instance,

$$\begin{aligned}\mathcal{C}(\gamma, x_0, k, \nu = 1) &= \text{Re}(\omega^{-1} \exp(\omega x_0) \Gamma(0, \omega x_0)) \\ \omega &= -ik + \gamma.\end{aligned}\quad (\text{A4})$$

Appendix B: Linear-in-Temperature Resistance

In this appendix we continue our discussion of systems whose resistance increases linearly with magnetic field. We make remarks of a more speculative nature arguing that these systems' resistance should increase linearly with temperature. We are continuing to assume that conduction is diffusive, with many scatterings, and that the spin triplet and the Zeeman term do not affect conduction. We are also continuing along the lines of Section III, attributing the long $\ln A$ tail of the loop area distribution to quantum coherence. Within this framework we examine the resistance's dependence on temperature.

As we have seen, the loop area distribution has a smooth logarithmic form with only two characteristic area scales: the UV cutoff A_0 , and the infrared cutoff A_{max} which regulates large loops. The ultraviolet cutoff

A_0 may be controlled by many length scales: the scattering length, the lattice spacing, the scale of the Fermi surfaces, and the crossover from WAL to WL which is controlled by the scales at which spin rotation symmetry and time reversal symmetry are broken, etc. These mechanisms depend weakly on temperature.

The main source of temperature dependence comes instead from the infrared cutoff A_{max} which regulates large loops. The tail of the $\ln A$ loop area distribution reflects quantum coherence. Regardless of which short distance physics controls the loop area distribution without quantum coherence, this physics has no control over quantum coherence, and therefore cannot determine the infrared cutoff A_{max} regulating the loop area distribution. The *only* mechanism available to limit the loop repetitions and thus supply a cutoff A_{max} on the loop area distribution's tail is quantum decoherence, which is controlled by temperature.

How does the IR cutoff A_{max} depend on temperature? Since in atomic units inverse temperature has units of area, it would be natural for $A_{max} \propto T^{-1}$ to scale inversely with temperature. We have already noted that $A_{max} \propto T^{-1}$ does obtain in the specific case of SdH oscillations.²⁹ It also holds in 2-D diffusive systems when the dominant mechanism of decoherence is through electron-electron interactions.^{61,62} In linear resistance systems $A_{max} \propto T^{-1}$ scaling should be very robust because the loop areas in the tail are so large that T^{-1} is the only area scale large enough match them.

If the decoherence area $A_{max} \propto T^{-1}$ scales inversely with temperature, it is then a simple matter to show that at $B = 0$ the resistance must be linear in temperature. Most simply, the linear magnetoresistance is $R_{xx}(B) = \pi q_C B A_0$. When $B = 0$ the inverse area B^{-1} diverges. The only scale available to take the place of B^{-1} is T^{-1} , and plugging this into the magnetoresistance formula immediately gives linear in temperature resistance $R_{xx}(T) = \pi q_C T A_0$.

Going into more detail, the logarithmic loop area distribution is $G_{xx}(A) \approx -(\pi A_0)^{-1} \ln|A|$. This should be regularized to give positive values because, as we have seen, in WL/WAL the Cooperon does not carry phase information and all Cooperon loop trajectories carry the same weight with the same sign. One possible regularization is to add $(\pi A_0)^{-1} \ln|A_{max}|$. Setting $B = 0$ and integrating with respect to area gives $R_{xx}(B = 0) \approx \pi A_0 / A_{max} \propto \pi A_0 T$ for $A_0 \ll A_{max} \propto T^{-1}$, plus regularization-dependent terms which are sensitive to the cutoffs. When $A_{max} \propto T^{-1}$ is comparable to A_0 the linear dependence on T collapses. At smaller temperatures the linear in temperature resistance is robust because B^{-1} and T^{-1} both act at large length scales and therefore are roughly interchangeable.

We summarize these mathematical arguments in three experimental observables:

- α is the coefficient of linear temperature dependence, i.e. $R(B = 0, T) = \alpha k_B T$.

- β is the coefficient of linear field dependence, i.e. $R(T=0, B) = \beta \mu_B B$.
- $\gamma = \alpha/\beta$ is the ratio of the coefficient of temperature dependence to the coefficient of field dependence.

These observables have the values

$$\begin{aligned}\alpha &= \pi A_0 / (A_{max} T) \\ \beta &= \pi q_C \mu_B^{-1} A_0 \\ \gamma &= q_C^{-1} \mu_B / (A_{max} T)\end{aligned}\quad (B1)$$

where $\mu_B = 1/2$ and $q_C = 2$ are the Bohr magneton and the Cooperon charge.

We can go a step further by combining the Heisenberg uncertainty relation with a $p^2/2m$ dispersion: $A_{max} = \langle (\Delta x)^2 \rangle = \hbar^2 / \langle p^2 \rangle$, where the momentum scale is determined by $\langle p^2 / 2(m_C/m_e) \rangle = T$, m_C is the Cooperon mass, and m_e is the electron mass. This produces $A_{max} T = m_e / 2m_C$. The Heisenberg relation used here is a quantum mechanical upper bound on the decoherence scale which can be obtained at a given temperature.

Using this relation gives:

$$\begin{aligned}\alpha &= 4\pi \frac{m_C}{2m_e} A_0 = \gamma \times 4\pi A_0 \\ \beta &= \pi q_C \mu_B^{-1} A_0 = 4\pi A_0 \\ \gamma &= \frac{2m_C \mu_B}{q_C m_e} = \frac{m_C}{2m_e}\end{aligned}\quad (B2)$$

These arguments indicate that γ 's physical meaning is simply the ratio of the Cooperon mass to that of two electrons, i.e. $\gamma = m_C / 2m_e$. When $\gamma = 1$ the coefficients α and β of both the linear-in-temperature resistance and the linear magnetoresistance are direct measures of the UV cutoff A_0 , with $R_{xx}(B=0) = \alpha T = 4\pi A_0 T$ and $R_{xx}(T=0) = \beta \mu_B B = 2\pi A_0 B$.

1. Relation to Bad Metals

Our derivation of linear-in-temperature resistance was made based on assumptions about diffusive scattering and the absence of spin physics. These assumptions hold in disordered topological insulators, but in many other materials they may not be valid. Nonetheless the linear-in-temperature resistance predicted here is also seen in high T_c superconductors (cuprates and pnictides) at temperatures above the superconducting phase. These strongly correlated materials display a resistance which increases linearly with temperature and does not saturate.⁶³ This linear dependence is inconsistent both with the WAL signal which increases much more slowly with T (logarithmically in 2-D and as a square root in 3-D) and with phonon based scattering which should saturate at a maximum determined by the atomic spacing. Materials whose resistance is linear in temperature are called bad metals and are understood to be strongly

correlated, but the details of the conduction process responsible for linear resistance are not understood. It is widely believed that linear-in-temperature resistance is correlated with high- T_c superconductivity. Very recently the linear dependence on temperature has been linked to linear magnetoresistance found in the same bad metal regime.^{64–66}

Most work on linear resistance in bad metals neglects the quantum interference contributions to electronic conduction which are responsible for WL/WAL. Linear resistance in bad metals extends up to temperatures of 1000 Kelvin, where it seems unreasonable for quantum coherence to play a role. Most work lays the responsibility for linear resistance with a momentum relaxation time scale τ which varies inversely with temperature. At large temperatures this time scale becomes very short, opening up a range of questions about correlation effects at short time scales⁶³, as well as the puzzling consequence that τ can be smaller than \hbar/E_F , where E_F is the Fermi energy.⁶⁷ Explanations of linear in temperature resistance have been given using resonating-valence-bond theory⁶⁸, marginal Fermi liquids⁶⁹, hydrodynamics of quantum critical liquids⁷⁰, the SYK model with effective medium theory⁷¹, and bounds on diffusion in incoherent metals⁶⁷. In Refs.^{68–70} the momentum relaxation time $\tau \propto T^{-1}$ scales inversely with temperature, and therefore simple formulas such as the Drude formula which have $\rho \propto \tau^{-1}$ produce linear in temperature resistance. Quantum interference is omitted from these simple estimates of the resistance. Ref.⁶⁷ follows a similar argument but instead of τ uses a time scale $\tau_{eff} \propto T^{-1}$ which controls diffusion. Ref.⁷¹ computes the resistance from the leading order term in Boltzmann theory, with a self-energy $\Sigma \propto \tau^{-1}$ which is linear in T . The one thing in common between these works and the results presented in the present paper is that the source of linear resistance is not attributed to quantities at the atomic length scale, such as the band structure.

We list some arguments for not using the present paper's calculations as an explanation of linear resistance in bad metals:

- Many believe that scattering in bad metals is so strong, and the temperatures of up to 1000 Kelvin are so large, that linear resistance cannot rely on quantum interference or quantum coherence. Instead bad metals are in a regime of incoherent, short lived excitations, and strong dephasing.
- Many believe that bad metals are not Fermi liquids; that their carriers and excitations are not fundamental (bare) electrons and holes. Nor can they be (adiabatically) mapped to bare fermions. Therefore it would be surprising to many if bare electrons and holes and their pairs (Cooperons) were to play a determining role in conduction.
- Given this doubt, it is difficult to distinguish between spin-singlet and spin-triplet components of

the Cooperon, or to use reasoning about the singlet and triplet to decide whether spin has a role in conduction.

- The spin physics of bad metals may be extremely rich, both in experimental signatures such as magnon spectra, and in the many theories of bad metals and high- T_c superconductivity. It is difficult to exclude the possibility that spin has a role in conduction in bad metals.
- The theory of diffusons and Cooperons, of weak localization and weak antilocalization, generally assumes that the scattering centers are static and that scattering is elastic; it conserves energy. Moreover the diffusive conduction discussed in the present paper requires a substantial density of scatterers. In contrast, static disorder does not seem to be a salient feature of bad metals. Instead inelastic scattering caused by interactions is the key.

In the face of these arguments it is necessary to review the assumptions that went into the present paper. Certainly scattering is strong in bad metals, putting them in the diffusive regime - though the scatterers are dynamic not static. The real problem with this paper's assumptions is the requirement that spin physics does not play a role in conduction. Because of this difficulty, we can not be sure of the transformation from field to loop area distribution; we can not be sure that the loop areas in bad metals follow a $\ln A$ distribution.

If we were able to exclude spin effects on conduction, then the arguments of this paper would proceed inexorably, with all the rigor of charge conservation, gauge invariance, and quantum field theory, and arrive at the $\ln A$ loop area distribution. At this point we would have to confront the difficulty that the A figuring in the $\ln A$ is the sum of areas of a vast number of strongly interacting electron-hole pairs; it is not the area of a single non-interacting random walker. Therefore perhaps the $\ln A$ loop distribution is caused by strongly interacting physics, not by simple random walks. This difficulty in interpreting the $\ln A$ distribution may complicate the relation between temperature and the IR cutoff, and thus impede our arrival at linear in temperature resistance. On the other hand $A_{max} \propto T^{-1}$ is dimensionally correct, and a large area scale like T^{-1} is necessary to explore the tail of the $\ln A$ distribution. Therefore we may arrive at linear-in-temperature resistance, even if the $\ln A$ loop area distribution is caused by strong interactions and not Cooperons.

2. Experimental Results in Bad Metals

Bearing in mind the difficulties discussed in the previous paragraphs, we comment on a few interesting experiments. First, Hayes et al measured $\gamma = \alpha/\beta$, where

α is the coefficient of linear-in-temperature dependence and β is the coefficient of linear-in-field dependence.⁶⁴ γ was measured in the high- T_c pnictide superconductor $\text{BaFe}_2(\text{As}_{1-x}\text{P}_x)_2$ at dopings ranging between 0.31 and 0.41. It was found to be identical to one in atomic units, within the experimental error bar of 7%. Further studies of the cuprate $\text{La}_{2-x}\text{Sr}_x\text{CuO}_4$ and of $\text{Yb}_{1-x}\text{La}_x\text{Rh}_2\text{Si}_2$ at various dopings near optimal doping have found constants between 0.7 and 2.3.^{64,72} We conclude that γ does depend on the host material, but only mildly, and that it is of order 1. If our formula $\gamma = m_C/2m_e$ is correct, then experimental observation of $\gamma = 1$, i.e. a $p^2/2m_e$ dispersion, implies that in the compounds studied by Refs.^{64,72} the carriers responsible for linear resistance have mass $m_C = 2m_e$ equal to twice the bare electron mass m_e , and are insensitive to mass renormalization via band structure and other effects.

We examine the UV cutoff A_0 's scaling in several cuprates analyzed by Ref.⁷³, which determined the linear coefficient α in $\text{La}_{2-x}\text{Sr}_x\text{CuO}_4$ (LSCO), $\text{YBa}_2\text{Cu}_3\text{O}_{6+\delta}$ (YBCO), $\text{Tl}_2\text{Ba}_2\text{CuO}_{6+\delta}$ (Tl2201), and $\text{HgBa}_2\text{CuO}_{4+\delta}$ (Hg1201). Ref.⁷³ found that α - the coefficient of linear-in-temperature resistance - is the same in all four compounds if one uses the sheet resistance per CuO_2 plane, not per unit cell. They also found that α is inversely proportional to the doping p for $p \leq 0.20$, where p is the number of holes per unit cell, not per CuO_2 plane. After conversion to atomic units one finds that $\alpha = \pi \times 64 a_0^2 \times p^{-1}$.⁸⁰

We surmise on dimensional grounds that α should not depend on the doping, but instead on the 2-D carrier density ρ_{2D} . Using $p = \rho_{2D} \times \mathcal{A}$ where $\mathcal{A} \approx 53a_0^2$ is the cross-section of the unit cell in the cuprates' copper oxide plane, we arrive at $R_{xx}(B=0) = 0.30 \times 4\pi \times T \times \rho_{2D}^{-1}$.

Comparison to our formula where $R_{xx}(B=0, T) = 4\pi\gamma \times A_0 T$ suggests that in these compounds the UV cutoff A_0 of the loop area distribution is the inverse of the carrier density, i.e. $A_0 = \rho_{2D}^{-1}$.⁸¹ This offers the possibility of determining the charge carrier density directly from either the linear magnetoresistance or the linear in temperature resistance, without any speculation about the compound's chemistry or band structure.

Acknowledgments

We gratefully acknowledge formative and stimulating discussions with S. Kettemann, A. Leggett, Y. Li, C. Lin, X. Dai, V. Dobrosavljevic, H.-J. Lee, Q. Wu, T. Ohtsuki, J. Zaanen, K. Schalm, T. Takimoto, K.-S. Kim, X. Wan, P. Niklowitz, A. Ho, J. Saunders, L. Levitin, J. Koelzer, T. Schapers, H. Luth, C. Weyrich, P. Hasnip, A. Kim, M. Ma, P. Coleman, S. Hayden, I. Bozovic, P. Abbamonte, and G. Parisi. We also thank especially A. Petrovic who discussed the manuscript during preparation. **Funding:** We acknowledge support from EPSRC grant EP/M011038/1.

-
- * Electronic address: vincent@sacksteder.com
- ¹ S. X. Zhang, R. D. McDonald, A. Shekhter, Z. X. Bi, Y. Li, Q. X. Jia, and S. T. Picraux, *Applied Physics Letters* **101**, 202403 (2012).
 - ² W. Zhang, R. Yu, W. Feng, Y. Yao, H. Weng, X. Dai, and Z. Fang, *Phys. Rev. Lett.* **106**, 156808 (2011).
 - ³ X. Wang, Y. Du, S. Dou, and C. Zhang, *Phys. Rev. Lett.* **108**, 266806 (2012).
 - ⁴ J. Feng, Y. Pang, D. Wu, Z. Wang, H. Weng, J. Li, X. Dai, Z. Fang, Y. Shi, and L. Lu, *Phys. Rev. B* **92**, 081306 (2015).
 - ⁵ F. Kisslinger, C. Ott, C. Heide, E. Kampert, B. Butz, E. Spiecker, S. Shallcross, and H. B. Weber, *Nature Physics* **11**, 650 (2015).
 - ⁶ C. Zhang, C. Guo, H. Lu, X. Zhang, Z. Yuan, Z. Lin, J. Wang, and S. Jia, *Phys. Rev. B* **92**, 041203 (2015).
 - ⁷ K. Wang, D. Graf, and C. Petrovic, *Phys. Rev. B* **89**, 125202 (2014).
 - ⁸ X. Xu, W. H. Jiao, N. Zhou, Y. Guo, Y. K. Li, J. Dai, Z. Q. Lin, Y. J. Liu, Z. Zhu, X. Lu, et al., *Journal of Physics: Condensed Matter* **27**, 335701 (2015).
 - ⁹ Y. Sun, S. Pyon, and T. Tamegai, *Phys. Rev. B* **93**, 104502 (2016).
 - ¹⁰ Y. Tanabe, K. K. Huynh, S. Heguri, G. Mu, T. Urata, J. Xu, R. Nouchi, N. Mitoma, and K. Tanigaki, *Phys. Rev. B* **84**, 100508 (2011).
 - ¹¹ D. Bhoi, P. Mandal, P. Choudhury, S. Pandya, and V. Ganesan, *Applied Physics Letters* **98**, 172105 (2011).
 - ¹² J. Fenton and A. J. Schofield, *Phys. Rev. Lett.* **95**, 247201 (2005).
 - ¹³ A. E. Koshelev, *Phys. Rev. B* **88**, 060412 (2013).
 - ¹⁴ A. A. Abrikosov, *Phys. Rev. B* **58**, 2788 (1998).
 - ¹⁵ T. Khouri, U. Zeitler, C. Reichl, W. Wegscheider, N. E. Hussey, S. Wiedmann, and J. C. Maan, *Phys. Rev. Lett.* **117**, 256601 (2016).
 - ¹⁶ M. M. Parish and P. B. Littlewood, *Nature* **426**, 162 (2003).
 - ¹⁷ R. Winkler, *Spin-orbit coupling effects in two-dimensional electron and hole systems*, vol. 191 (Springer, 2003).
 - ¹⁸ L. Schäfer and F. Wegner, *Zeitschrift für Physik B Condensed Matter* **38**, 113 (1980).
 - ¹⁹ K. Efetov, *Supersymmetry in disorder and chaos* (Cambridge University Press, 1999).
 - ²⁰ S. Hikami, A. I. Larkin, and Y. Nagaoka, *Progress of Theoretical Physics* **63**, 707 (1980).
 - ²¹ G. Bergman, *Phys. Rev. Lett.* **48**, 1046 (1982), URL <https://link.aps.org/doi/10.1103/PhysRevLett.48.1046>.
 - ²² J. Chen, X. Y. He, K. H. Wu, Z. Q. Ji, L. Lu, J. R. Shi, J. H. Smet, and Y. Q. Li, *Phys. Rev. B* **83**, 241304 (2011), URL <https://link.aps.org/doi/10.1103/PhysRevB.83.241304>.
 - ²³ R. P. Feynman and A. R. Hibbs, *Quantum mechanics and path integrals* (McGraw-Hill, 1965).
 - ²⁴ J. Rammer, *Quantum transport theory* (CRC Press, 2018).
 - ²⁵ K. G. Wilson, *Phys. Rev. D* **10**, 2445 (1974).
 - ²⁶ R. P. Feynman, *Phys. Rev.* **80**, 440 (1950).
 - ²⁷ A. Ashtekar and C. Rovelli, *Classical and Quantum Gravity* **9**, 1121 (1992).
 - ²⁸ L. Onsager, *The London, Edinburgh, and Dublin Philosophical Magazine and Journal of Science* **43**, 1006 (1952).
 - ²⁹ B. Laikhtman and E. L. Altshuler, *Annals of Physics* **232**, 332 (1994).
 - ³⁰ B. L. Altshuler and A. G. Aronov, *JETP Lett.*, **33**, 499 (1981).
 - ³¹ V. K. Dugaev and D. E. Khmel'nitskii, *Sov. Phys. JETP* **59**, 1038 (1984).
 - ³² G. Bergmann, *Phys. Rev. B* **39**, 11280 (1989).
 - ³³ O. E. Raichev and P. Vasilopoulos, *Journal of Physics: Condensed Matter* **12**, 589 (2000).
 - ³⁴ J. S. Meyer, A. Altland, and B. L. Altshuler, *Phys. Rev. Lett.* **89**, 206601 (2002).
 - ³⁵ I. Garate and L. Glazman, *Phys. Rev. B* **86**, 035422 (2012).
 - ³⁶ C. W. J. Beenakker and H. van Houten, *Phys. Rev. B* **38**, 3232 (1988).
 - ³⁷ C. J. Lin, X. Y. He, J. Liao, X. X. Wang, V. S. IV, W. M. Yang, T. Guan, Q. M. Zhang, L. Gu, G. Y. Zhang, et al., *Phys. Rev. B* **88**, 041307 (2013).
 - ³⁸ V. E. Sacksteder, K. B. Arnardottir, S. Kettemann, and I. A. Shelykh, *Phys. Rev. B* **90**, 235148 (2014).
 - ³⁹ Q. Wu and V. E. Sacksteder, *Phys. Rev. B* **90**, 045408 (2014).
 - ⁴⁰ K. Nomura, M. Koshino, and S. Ryu, *Phys. Rev. Lett.* **99**, 146806 (2007).
 - ⁴¹ J. H. Bardarson, J. Tworzydło, P. W. Brouwer, and C. W. J. Beenakker, *Phys. Rev. Lett.* **99**, 106801 (2007).
 - ⁴² C. H. Lewenkopf, E. R. Mucciolo, and A. H. Castro Neto, *Phys. Rev. B* **77**, 081410 (2008).
 - ⁴³ G. M. Minkov, A. V. Germanenko, V. A. Larionova, S. A. Negashev, and I. V. Gornyi, *Phys. Rev. B* **61**, 13164 (2000), URL <https://link.aps.org/doi/10.1103/PhysRevB.61.13164>.
 - ⁴⁴ D. V. Baxter, R. Richter, M. L. Trudeau, R. W. Cochrane, and J. O. Strom-Olsen, *Journal de Physique* **50**, 1673 (1989).
 - ⁴⁵ A. P. Dmitriev, V. Y. Kachorovskii, and I. V. Gornyi, *Phys. Rev. B* **56**, 9910 (1997), URL <https://link.aps.org/doi/10.1103/PhysRevB.56.9910>.
 - ⁴⁶ V. Gasparyan and A. Y. Zyuzin, *Sov. Phys. Solid State* **27**, 999 (1985).
 - ⁴⁷ M. Dyakonov, *Solid state communications* **92**, 711 (1994).
 - ⁴⁸ A. Cassam-Chenai and B. Shapiro, *Journal de Physique I* **4**, 1527 (1994).
 - ⁴⁹ K. Ishii, *Progress of Theoretical Physics Supplement* **53**, 77 (1973).
 - ⁵⁰ B. Simon and T. Spencer, *Communications in Mathematical Physics* **125**, 113 (1989).
 - ⁵¹ C. W. J. Beenakker, *Rev. Mod. Phys.* **69**, 731 (1997), URL <https://link.aps.org/doi/10.1103/RevModPhys.69.731>.
 - ⁵² T. Ando and H. Suzuura, *Journal of the Physical Society of Japan* **71**, 2753 (2002).
 - ⁵³ Y. Takane, *Journal of the Physical Society of Japan* **73**, 1430 (2004).
 - ⁵⁴ B. L. Altshuler, A. G. Aronov, and B. Z. Spivak, *JETP Lett.* **33**, 94 (1981).
 - ⁵⁵ V. E. Sacksteder and Q. Wu, *Phys. Rev. B* **94**, 205424 (2016).
 - ⁵⁶ L. Oroszlány, P. Rakyta, A. Kormányos, C. J. Lambert, and J. Cserti, *Phys. Rev. B* **77**, 081403 (2008).
 - ⁵⁷ T. K. Ghosh, A. De Martino, W. Häusler, L. Dell'Anna, and R. Egger, *Phys. Rev. B* **77**, 081404 (2008).
 - ⁵⁸ J. R. Williams and C. M. Marcus, *Phys. Rev. Lett.* **107**, 046602 (2011).
 - ⁵⁹ K. Fujita, C. K. Kim, I. Lee, J. Lee, M. H. Hamidian, I. A. Firmo, S. Mukhopadhyay, H. Eisaki, S. Uchida, M. J.

- Lawler, et al., *Science* **344**, 612 (2014).
- ⁶⁰ Q. Wu, L. Du, and V. E. Sacksteder, *Phys. Rev. B* **88**, 045429 (2013).
- ⁶¹ B. L. Altshuler, A. G. Aronov, and D. E. Khmelnitskii, *J. Phys. C: Solid State Phys.* **15**, 7367 (1982).
- ⁶² S. Matsuo, K. Chida, D. Chiba, T. Ono, K. Slevin, K. Kobayashi, T. Ohtsuki, C.-Z. Chang, K. He, X.-C. Ma, et al., *Phys. Rev. B* **88**, 155438 (2013), URL <https://link.aps.org/doi/10.1103/PhysRevB.88.155438>.
- ⁶³ N. E. Hussey, K. Takenaka, and H. Takagi, *Philosophical Magazine* **84**, 2847 (2004).
- ⁶⁴ I. M. Hayes, R. D. McDonald, N. P. Breznay, T. Helm, P. J. Moll, M. Wartenbe, A. Shekhter, and J. G. Analytis, *Nature Physics* **12**, 916 (2016).
- ⁶⁵ P. Giraldo-Gallo, J. Galvis, Z. Stegen, K. Modic, F. Balakirev, J. Betts, X. Lian, C. Moir, S. Riggs, J. Wu, et al., *Science* **361**, 479 (2018).
- ⁶⁶ R. Kumar, S. Singh, and S. Nair, *arXiv preprint arXiv:1801.03768* (2018).
- ⁶⁷ S. A. Hartnoll, *Nature Physics* **11**, 54 (2015).
- ⁶⁸ N. Nagaosa and P. A. Lee, *Phys. Rev. Lett.* **64**, 2450 (1990).
- ⁶⁹ C. M. Varma, P. B. Littlewood, S. Schmitt-Rink, E. Abrahams, and A. E. Ruckenstein, *Phys. Rev. Lett.* **63**, 1996 (1989), URL <https://link.aps.org/doi/10.1103/PhysRevLett.63.1996>.
- ⁷⁰ R. A. Davison, K. Schalm, and J. Zaanen, *Phys. Rev. B* **89**, 245116 (2014), URL <https://link.aps.org/doi/10.1103/PhysRevB.89.245116>.
- ⁷¹ A. A. Patel, J. McGreevy, D. P. Arovas, and S. Sachdev, *Phys. Rev. X* **8**, 021049 (2018), URL <https://link.aps.org/doi/10.1103/PhysRevX.8.021049>.
- ⁷² P. Giraldo-Gallo, J. A. Galvis, Z. Stegen, K. A. Modic, F. F. Balakirev, J. B. Betts, X. Lian, C. Moir, S. C. Riggs, J. Wu, et al., *arXiv preprint arXiv:1705.05806* (2017).
- ⁷³ N. Barišić, M. K. Chan, Y. Li, G. Yu, X. Zhao, M. Dressel, A. Smontara, and M. Greven, *Proceedings of the National Academy of Sciences* **110**, 12235 (2013).
- ⁷⁴ G. P. Mikitik and Y. V. Sharlai, *Phys. Rev. Lett.* **82**, 2147 (1999).
- ⁷⁵ A. J. Leggett, *Quantum liquids: Bose condensation and Cooper pairing in condensed-matter systems* (Oxford University Press, 2006).
- ⁷⁶ T. Hu, Y. Liu, H. Xiao, G. Mu, and Y.-f. Yang, *Scientific reports* **7**, 9469 (2017).
- ⁷⁷ A slightly different result $\cos(A/NA^F)$ obtains for the N -th Landau level of Dirac fermions.⁷⁴
- ⁷⁸ To verify that loop area distribution for Landau levels and SdH oscillations decays exponentially, we numerically Fourier transformed the conductance formulas in Ref.²⁹, because analytical formulas for the Fourier transform of this signal are not available.
- ⁷⁹ At very strong magnetic fields, when the magnetic length $\sqrt{\hbar c/eB}$ is compared with the mean free path, there is a further transition to $G_{xx} \propto 1/\sqrt{B}$ behavior.^{45–48}
- ⁸⁰ Up to the multiplicative constant, this formula $R \propto T/p$ is the same as Ref.⁶⁸'s RVB result. See also Ref.⁷⁵ for discussion of the resistance per CuO_2 plane.
- ⁸¹ Ref.⁷⁶ has argued that the linear coefficient of the resistivity dR/dT is proportional to λ_L^2 across a range of cuprate, pnictide, and heavy fermion materials, where λ_L is the London penetration depth. Since both Ref.⁷⁶ and Ref.⁷³ analyze the same data on LSCO, this suggests a scaling relationship between λ_L^2 and the inverse carrier density ρ_{2D}^{-1} .